INTERNATIONAL JOURNAL OF INNOVATIVE RESEARCH & DEVELOPMENT

ISSN 2278 – 0211 (Online)

Photocatalytic Degradation of Dye Acid Orange Seven on Titanium Dioxide Photocatalysts Immobilized on Stainless Steel Coated Layers: Role of Catalyst Loading and Ultrasonic Treatment

Patrick Kimutai Tum
Lecturer, Department of Chemistry, University of Nairobi, Nairobi, Kenya

Abstract:
Supported titanium dioxide (TiO_2) was investigated for potential application in photocatalytic degradation of dye acid Orange 7 in textile wastewater. Two commercial powder photocatalysts, Degussa (P25) and Precheza (AV01), were immobilized on stainless steel plates of dimensions (75 mm × 25 mm) through Electrophoretic Deposition Process (EPD) from aqueous colloidal suspensions of n-TiO_2, c=10 g.L^{-1} produced in methanol. Two sets of coated layers were prepared - using ultrasonically treated TiO_2 colloidal suspensions and without ultrasonic treatment. The prepared coated layers were fitted onto a four-hole photocatalytic reactor operating under batch-mode conditions. As a source of UV light, Sylvania LynxS, 11W UV lamps emitting light of wavelength between 320-400 nm with maximum wavelength at λ=355 nm was used. The current study aimed to evaluate the effect of ultrasonic treatment on the catalyst's colloidal suspension and electrophoretic deposition loading (mg/cm^2) on its surface area on the resultant photocatalytic degradation of dye Acid Orange 7. The photocatalytic degradation of the dye was monitored by changes in dye absorbance for 120 minutes at an interval of 30 minutes. Changes in dye concentration were determined by ultraviolet spectrophotometry at λ = 485 nm. The initial concentration of dye Acid Orange 7 used in the experiments was c=1×10^{-4} mol. L^{-1}. The findings show that 61.1 % of dye mineralization was achieved after 120 minutes of photocatalytic degradation. The optimum catalytic loading for maximum photocatalytic degradation was determined at 0.75 mg/cm^2 for the two commercial powder catalysts - TiO_2 (P25/AV01) in ultrasonically treated TiO_2 (P25) and non-ultrasonically treated TiO_2 (AV01). Ultrasonic treatment of TiO_2 (P25) colloidal suspensions before immobilisation positively influenced its photocatalytic activity, whereas ultrasonic treatment negatively affected the photoactivity of TiO_2 (AV01). Overall, TiO_2 (AV01) proved to be more efficient by 28.6%, compared to TiO_2 (P25). The results show the potential application of UV-TiO_2 treatment model in the remediation of coloured dye Acid Orange textile wastewater.

Keywords: *Dye acid Orange seven, titanium dioxide, ultrasonic treatment, catalyst loading, photocatalytic reactor*

1. Introduction

1.1. Overview Advanced Oxidation Processes (AOPs)

The photocatalytic degradation mechanism is dependent on Ultra Violet light (UV), in the form of a photon (hv), with energy equal to or higher than the band gap energy (E_g) falling on the surface of a powder semi-conductor catalyst exciting electrons from the valency band to conduction band (Cabanas-Polo & Boccaccini, 2015). This leads to the generation of electron/hole (e^-/h^+) pairs with free electrons in the empty conduction band, leaving an electron vacancy/hole in the valency band (Ajmal *et al.,* 2014; Mohan *et al.,* 2012). Under UV light illumination and an ideal semi-conductor photocatalyst, electron/hole pairs with free electrons are generated in the unfilled conduction band, leaving positively charged holes (h^+) in the valence band (Mohan *et al.,* 2012). The formation of these holes in the valency allows adsorbed water to be oxidised to strong (•OH) radicals whose strong oxidative species (2.8 V vs. SHE) oxidises a majority of organic compounds (Muruganadham *et al.,* 2014). The organic intermediates formed are oxidized by O_2 or (•OH) radicals and mineralized to CO_2 and H_2O as the final products (Hussein & Abass, 2010). Hydroxyl radicals (•OH) are strong oxidizing species that react rapidly with most electron-rich sites of organic contaminants (Bergamini *et al.,* 2009). These electron-hole pairs initiate a series of chain reactions that mineralize organic pollutants to carbon dioxide and water (Wojnarovits & Takacs, 2008). The reactions involve cleavaging the conjugated carbon-carbon double bonds found in polyphenols by (•OH) radicals, causing decolourization of coloured wastewater (Cernigoj, 2007; Bizani *et al.,* 2006). This technique prevents sludge formation, avoiding secondary pollution (Pelaez *et al.,* 2012; Gogate & Pandit, 2004). Photocatalytic degradation reactions eliminate from wastewater all categories of organic contaminants (Farnoush *et al.,* 2012; Cernigoj, 2007). Its applications in slurry-type suspensions are limited due to limitations caused by difficult catalyst

separation after photocatalytic degradation reactions (Thiruvenkatachari *et al.,* 2008; Cordero-Arias *et al.,* 2013). The development of knowledge in semi-conductor electrochemistry has led to rapid growth in the field of photocatalysis (Dor *et al.,* 2009).

1.2. Application of Tio_2 as a Semi-Conductor Photocatalyst

Titanium dioxide as a semi-conductor has been successfully used as a photocatalyst for the oxidative degradation of organic compounds, including dyes (Gaya & Abdulla, 2008). The anatase modification is the most practical for photocatalytic environmental applications such as water purification, wastewater treatment, and water disinfections (Yousefipoura *et al.,* 2013; Cernigoj, 2007). It is biologically and chemically inert, stable regarding photo-corrosion, and chemical corrosion, and affordable. Its disadvantage is, however, too high band gap energy (about 3.2 eV) that allows titanium dioxide to absorb only UV light with a wavelength lower than $\lambda<388$ nm. This reduces the amount of solar energy absorbed by the catalyst down to 5% (Thiruvenkatachari *et al.,* 2008; Bizani *et al.,* 2006). The photogenerated holes (h^+) formed after the excitation of electrons (e^-) from the valence band to the conduction band exhibit strong oxidizing potential (Akpan & Hameed, 2009). The excited electrons are scavenged by oxygen and reduced to form superoxides from Dioxygen (Fujishima *et al.,* 2000). Fujishima *et al.* (2008) demonstrated the 'Honda-Fujishima effect' that involved the photochemical splitting of H_2O into H_2 and O_2 using TiO_2 semi-conductor photocatalyst. The photocatalytic degradation mechanism is illustrated in figure 1 below.

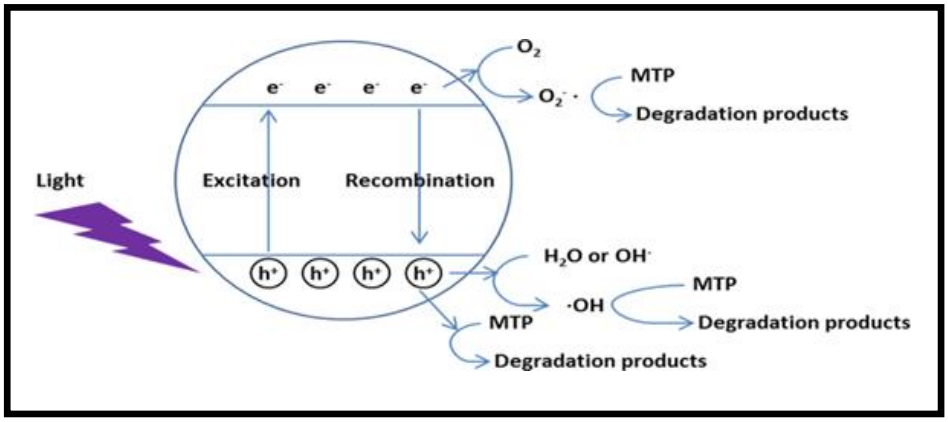

Figure 1: Photocatalytic Degradation Mechanism in Aqueous Dye Solutions (Cernigoj, 2007)

1.3. Experimental Design

1.3.1. Dye Studied, Formula and Physical Properties

Dye Acid Orange 7, an azo dye, is an orange-red powder exhibiting high water solubility (40 $g.L^{-1}$). The dye was purchased from Saffron Exim and used in the chemical industry for the following operations; liquid dye for paper, wool silk, jute, and leather dying. The dye can also be used as an indicator and biological shading. The dye is stable at room temperature and pressure with a melting point of 164°C. The molecular formula of the dye is $C_{16}H_{11}N_2NaO_4S$, and the molecular weight is 350.32 $g.mol^{-1}$. The structural formula of the dye is shown in figure 2 below.

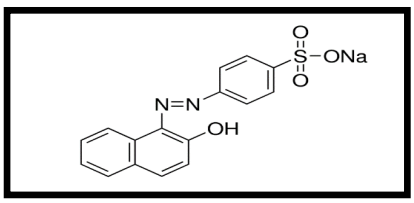

Figure 2: Structural Formula Acid Orange 7 (Bizani Et Al., 2006)

Figure 3: Acid Orange 7 Dye Powder (Saffron Exim)

1.3.2. Preparation of Stainless Steel Coated Tio_2 Layers – Cathodic Electrophoretic Deposition

Stainless steel plates of dimensions (75 mm × 25 mm) were used to immobilize TiO_2 powder catalysts (P25/AV01) using the Electrophoretic Deposition Process (EPD) from aqueous colloidal suspensions of n-TiO_2, 10 $g.L^{-1}$ produced in methanol. Two sets of coated layers were prepared - one using ultrasonically treated TiO_2 colloidal suspensions and a second without ultrasonic treatment. Water and methanol were used to prepare 500 mL of stable colloidal suspensions of concentration. The catalyst suspensions were pre-treated in an ultra-sound bath to:

- Break down particle agglomerates,
- Increase the surface area and create a uniform suspension suitable for Electrophoretic deposition (EPD)

The formation of bubbles during the deposition process was minimised by adding to the colloidal suspension a solution mixture of CH_3OH: H_2O (80:20). Using 500 mL round-bottomed flasks, the suspensions were magnetically stirred and treated ultrasonically for 60 seconds. Prior to deposition, the stainless steel plates (3 mm thickness) were initially polished to obtain a mirror finish before thoroughly being washed with distilled water, rinsed and ultrasonically degreased with acetone, and dried for 30 minutes in ambient air. The prepared stainless steel plates were weighed to obtain the mass of each layer used. The electrophoretic deposition of the catalyst suspension onto the plates was done at 4V.

During the deposition, electrode distance in the cell was maintained at a constant 10 mm. Electrophoretic deposition was done at the following time intervals: 5, 10, 30, and 60 seconds. The stainless steel coated layers were thereafter dried on ceramic tiles in ambient air at room temperature for 48 hours.

1.3.3. Photocatalytic Degradation Experiments UV-Tio_2

A stock solution of Acid Orange 7 dye $c=1.0\times10^{-4}$ $mol.L^{-1}$ was prepared by dissolving 0.037 g in 1000 mL of distilled water. The prepared stock solution was diluted to obtain the following dye solutions: (1×10^{-5} $mol.L^{-1}$, 2.5×10^{-5} $mol.L^{-1}$, 5×10^{-5} $mol.L^{-1}$, 7.5×10^{-5} $mol.L^{-1}$, 1×10^{-4} $mol.L^{-1}$). A full UV-Vis scan (200 nm - 800 nm) was done to evaluate the maximum absorption wavelength (λ_{max}). Dye solutions of v=25 mL were loaded into four cuvettes (v=30 mL) and placed onto the four-hole photocatalytic reactor set-up shown in figures 4 & 5 in section (2.1.3). The dye solutions were stirred using a magnetic stirrer at 1000 rpm to ensure a uniform reaction mixture. The solution was irradiated with Ultra Violet light of λ= 355 nm for a duration of 120 minutes using two Sylvania LynxS, 11W tubes that emitted UV light of wavelength between 320-400 nm. To determine a change in dye absorbance, after an interval of 30 minutes, 5 mL was drawn from each cuvette, and absorbance was measured using a UV/Vis spectrophotometer at λ_{max}= 485 nm. Thereafter, the dye solution was put back into the cuvette.

1.3.4. Four-Hole Photocatalytic Reactor

The photocatalytic reactor operated in batch mode, fitted with a thermostat to regulate the operating temperature at 25°C. Four 30 mL cuvettes were placed against four holes through which UV light λ =355 nm irradiated from two UV tubes of 11 W each. 25 mL of dye solution was loaded into each cuvette, irradiated with UV light, and stirred with a magnetic stirrer at 1000 rpm attached to the photocatalytic reactor. The stainless steel layers coated with TiO_2 catalyst were suspended into the cuvettes using metal clips, making contact with the dye solution, as shown in figures 4 & 5 below.

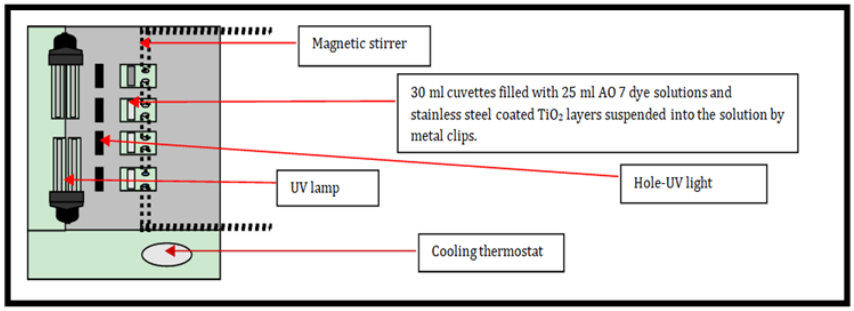

Figure 4: Four-Hole Photoreactor

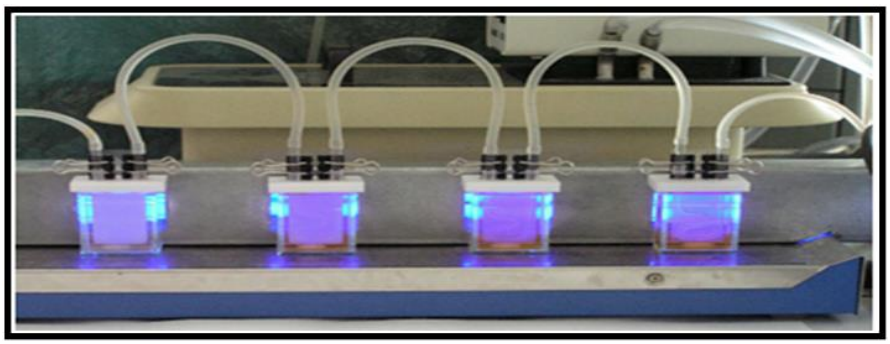

Figure 5: Four-Hole Photoreactor

1.4. Spectral Analysis

1.4.1. Maximum Absorption Wavelength (λ_{max})

A UV-Vis spectrophotometer (CECIL 2041) was used to determine the maximum absorption wavelength (λ_{max}) of the dye solution. One quartz cuvette (optical length 1 cm) was prepared for use by cleaning and drying using distilled water and dry linen tissue. This ensured that the transparent side remained clear, thereby eliminating interference as the UV light passed through the dye solution in the cuvette. The UV-Vis spectrophotometer was switched on and calibrated using distilled water in a quartz cuvette as a blank in the sample compartment, with the transparent sides facing the UV light source and the sample compartment lid closed. After calibration, dye absorption was recorded for various dye solution concentrations for full scans at (λ= 200-800 nm).

1.4.2. Molar Extinction Coefficient (ε) – Calibration curve

The molar extinction coefficient of dye Acid Orange 7 was derived from the Lambert-Beer law (A= εcl):

- A - Absorbance
- ε - molar absorption coefficient
- c - dye molar concentration (mol.L^{-1})
- l - optical path length (cm)

The coefficient was determined using a calibration curve plotted from absorbance values of dye Acid dye solutions of known concentrations. Serial solutions of dye Acid Orange were prepared as described in section (2.1.2) as follows; (1×10^{-5} mol.L^{-1}, 2.5×10^{-5} mol.L^{-1}, 5×10^{-5} mol.L^{-1} , 7.5×10^{-5} mol.L^{-1}, 1×10^{-4} mol.L^{-1}). The absorbance of these individual dye solutions was measured at λ=485 nm as determined in section (2.2.1) using a cuvette of optic length 1 cm and a UV-Vis Spectrophotometer. The molar extinction coefficient (ε) was determined by using the absorbance values obtained to plot a calibration curve using a linear extrapolation.

1.5. Objectives

The aims of the study were to:

- Evaluate the effect of TiO_2 catalyst loading (mg/cm^2) and ultrasonic treatment on the photocatalytic degradation of Acid Orange 7 dye,
- Determine the maximum absorption wavelength (λ_{max} for dye Acid Orange 7, and
- Measure the absorbance of five dye Acid Orange 7 solutions, calibrate the UV-Vis spectrophotometer, and determine the dye molar extinction coefficient (ε)

2. Results and Discussion

2.1. Spectral Properties of Dye Acid Orange 7

2.1.1. Maximum Absorption Wavelength (λ_{max})

The maximum absorption wavelength at (λ_{max}) for dye Acid Orange 7 (c=2.5×10^{-5} mol.L^{-1}) was determined by measuring absorbance between the wavelength λ= (200-800 nm) as indicated in figure 6 below.

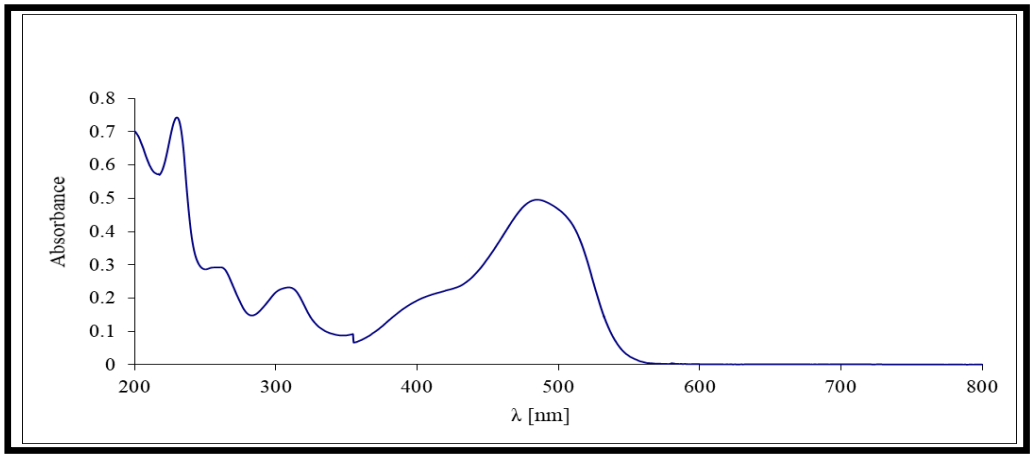

Figure 6: UV-Vis Spectra for Acid Orange 7

The results in figure 6 show the spectral properties of Acid Orange 7, i.e., maximum absorption wavelength at λ=485 nm, which lies within the UV region of Electromagnetic Spectrum (EM). We observe minimal dye absorption of visible (Vis) in the range between λ= (390-550 nm) and near-zero visible light absorption (Vis) between λ=550-800 nm.

2.1.2. Molar Extinction Coefficient (ε)

Figure 7 below shows the calibration curve plotted for dye Acid Orange to determine its molar extinction coefficient.

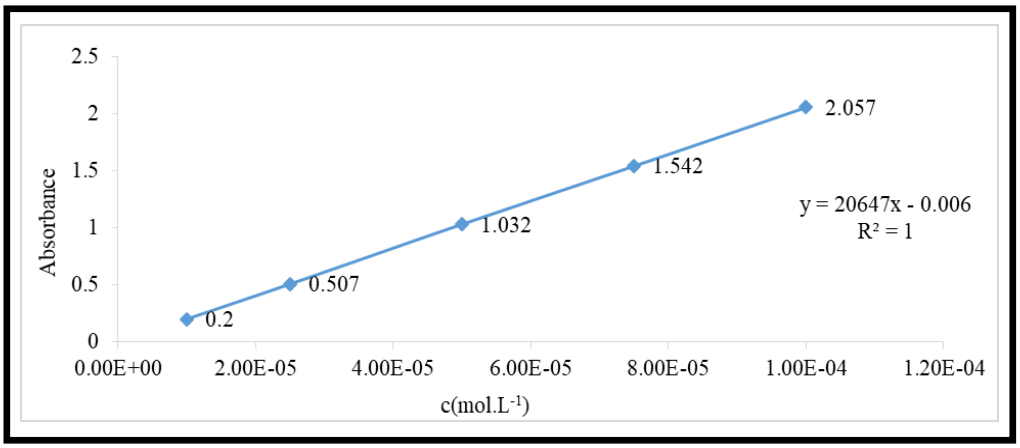

Figure 7: Calibaration Curve - Dye Acid Orange 7

The calibration curve for dye Acid Orange 7 was obtained by measuring the absorbance of dye solutions as described in (section 2.2.2). Maximum absorbance values were determined for each individual dye solution. A calibration curve was plotted using the absorbance values, as illustrated in figure 5. An experimental extinction coefficient value of 20647 $dm^{-3}.mol.^{-1}.cm^{-1}$ was calculated using the linear regression of the data obtained. This value indicates that Acid Orange 7 dye absorbs light efficiently at λ=485 nm, which lies in the UV region of the electromagnetic spectrum (EM).

2.2. Photocatalytic Degradation of Acid Orange 7 Dye – UV/Tio₂ (P25), with Ultrasonic Treatment

The effect of ultrasonic treatment of TiO_2 catalyst (P25) suspension and catalytic loading on photocatalytic degradation of Acid Orange 7 ($c=1\times10^{-4}$ mol. L^{-1}) dye is shown in figure 8 below.

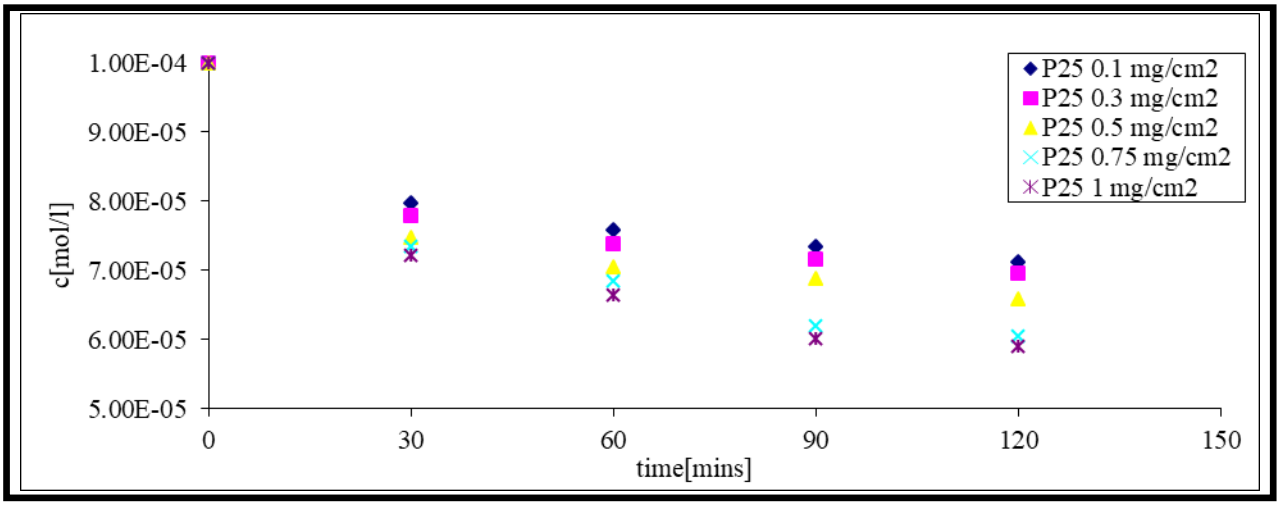

Figure 8: Photocatalytic Degradation of AO-7 Dye – UV/Tio₂ (P25), Ultrasonic Treatment

The results in figure 8 show an increase in TiO_2 (P25) catalyst loading in the range of 0.1 mg/cm2 -0.75 mg/cm^2 photocatalytic degradation of Acid orange 7 dye. At catalytic loading, 1 mg/cm^2, with ultrasonic treatment, dye photocatalytic degradation declined by 2.54% after 2 hours of treatment. The optimum catalyst loading with ultrasonic treatment was determined at 0.75 mg/cm^2, which resulted in a 9.84% increase in dye Acid Orange 7 photocatalytic degradation.

2.3. Photocatalytic Degradation of Acid Orange 7 Dye – UV/Tio₂ (P25), without Ultrasonic Treatment

The effect of TiO_2 catalyst (P25) catalytic loading without ultrasonic treatment on photocatalytic degradation of Acid Orange 7 ($c=1\times10^{-4}$ mol. L^{-1}) dye is shown in figure 9 below.

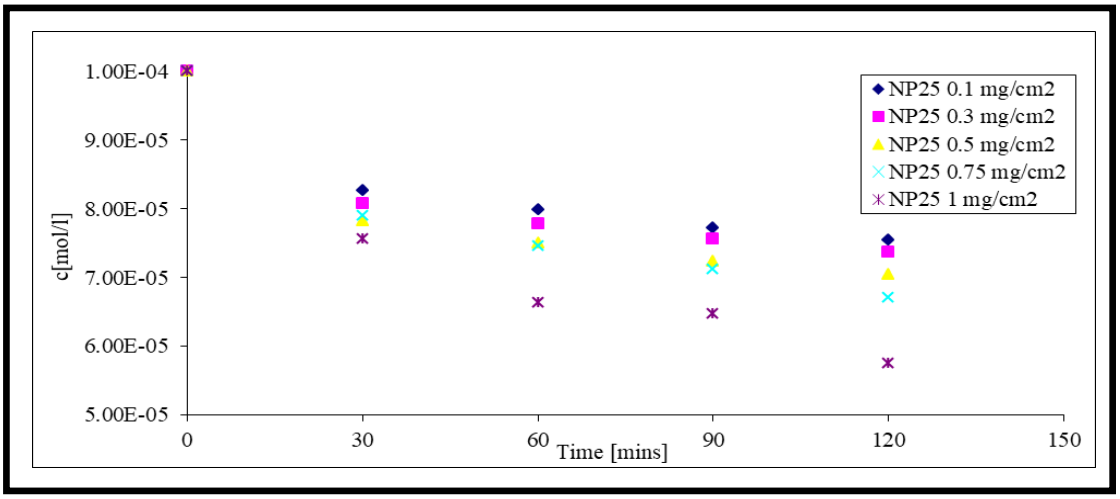

Figure 9: Photocatalytic Degradation of AO-7 Dye – UV/Tio₂ (P25), without Ultrasonic Treatment

Figure 9 shows that an increase in TiO_2 (P25) catalyst loading favoured dye Acid Orange photocatalytic degradation in the range 0.1 mg/cm2 – 0.75 mg/cm2. However, at catalyst loading 1 mg/cm^2, dye photocatalytic degradation declined by 2.52% without ultrasonic treatment. The optimum catalyst loading was determined at 0.75 mg/cm^2, which resulted in a 9.86% increase in dye Acid Orange photocatalytic degradation.

2.4. Photocatalytic Degradation of Acid Orange 7 Dye – UV/Tio₂ (AV01), Ultrasonic Treatment

The effect of ultrasonic treatment of TiO_2 catalyst (AV01) suspension and catalytic loading on photocatalytic degradation of Acid Orange 7 ($c=1\times10^{-4}$ mol. L^{-1}) dye is shown in figure 10 below.

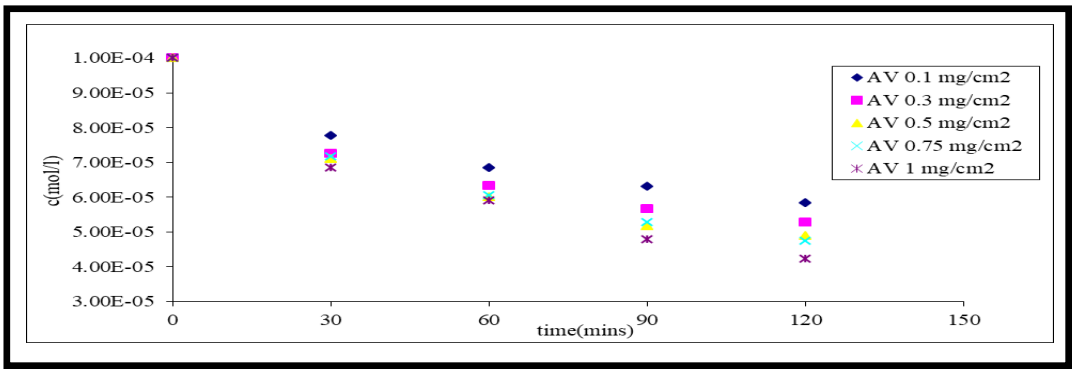

Figure 10: Photocatalytic Degradation of AO-7 dye – UV/TiO₂ (AV01), with Ultrasonic Treatment

From the results shown in figure 10, the photocatalytic degradation of dye Acid Orange 7 increased in the catalyst loading range 0.1 mg/cm^2 – 0.75 cm^2 with ultrasonic treatment. At TiO_2 (AV01) catalyst loading = 1 mg/cm^2, dye photocatalytic degradation increased by 0.236%. The optimum catalyst loading for TiO_2 (AV01) was determined to be 0.75 mg/cm^2 without ultrasonic treatment, which increased dye photocatalytic degradation by 6.75%. Overall, TiO_2 (AV01) catalyst, without ultrasonic treatment, showed increased dye Acid Orange 7 photocatalytic degradation by 4.56% compared to the ultrasonically treated TiO_2 (AV01) catalyst.

2.5. Photocatalytic Degradation of Acid Orange 7 Dye – UV/Tio₂ (AV01), without Ultrasonic Treatment

The effect of TiO_2 catalyst (AV01) catalytic loading without ultrasonic treatment on photocatalytic degradation of Acid Orange 7 ($c=1\times10^{-4}$ mol. L^{-1}) dye is shown in figure 11 below.

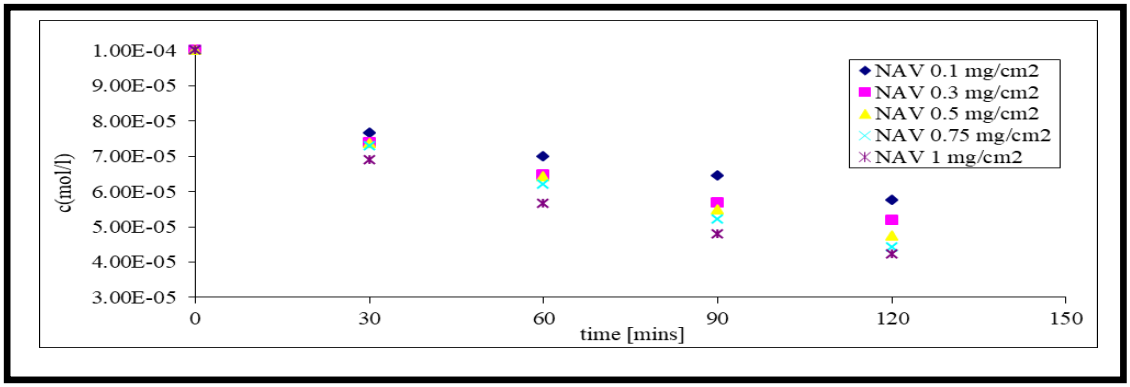

Figure 11: Photocatalytic Degradation of AO-7 Dye – UV/Tio₂ (AV01), without Sonication Pre-Treatment

The results in figure 11 show that in the catalyst loading range between 0.1 mg/cm² – 1 mg/cm², the photocatalytic degradation of dye Acid Orange 7 increased by 26,7%. At catalyst loading 1 mg/cm², the photocatalytic degradation increased marginally by 4.29%. From the results in figures 8 & 9, TiO_2 (AV01) ultrasonic treatment reveals a negative effect on dye Acid Orange 7 photocatalytic degradation.

3. Conclusions

The commercial TiO_2 photocatalysts (P25/AV01) used showed great potential for application as photocatalysts in the treatment of dye Acid Orange 7 textile wastewater. TiO_2 (AV01) catalyst showed better photocatalytic activity than TiO_2 (P25) by 28.6%. The optimum catalyst loading was determined at 0.75 mg/cm² for the two catalyst types. The ultrasonic treatment of aqueous catalyst colloidal suspensions preceding immobilization positively impacted the photocatalytic degradation potential of TiO_2 (P25) while unfavorably affecting TiO_2 (AV01).

4. References

i. Ajmal, A., Majeed, I., Malik, R. N., Idriss, H., & Nadeem, M. A. (2014). Principles and mechanisms of photocatalytic dye degradation on TiO2 based photocatalysts: A comparative overview. Rsc Advances, 4(70), 37003-37026.
ii. Akpan, U., & Hameed, B. (2009). Parameters affecting the photocatalytic degradation of dyes using TiO2-based photocatalysts: A review. Journal of hazardous materials, 170(2), 520-529.
iii. Bergamini, R. B., Azevedo, E. B., & De Araújo, L. R. R. (2009). Heterogeneous photocatalytic degradation of reactive dyes in aqueous TiO2 suspensions: Decolourisation kinetics. Chemical Engineering Journal, 149(1), 215-220.
iv. Bizani, E., Fytianos, K., Poulios, I., & Tsiridis, V. (2006). Photocatalytic decolourisation and degradation of dye solutions and wastewaters in the presence of titanium dioxide. Journal of hazardous materials, 136(1), 85-94.
v. Cernigoj, U. (2007). Photodegradation of organic pollutants in aqueous solutions catalyzed by immobilized titanium dioxide: Novel towards higher efficiency, dissertation nova Gorica.
vi. Fujishima, A., Rao, T. N., & Tryk, D. A. (2000). Titanium dioxide photocatalysis. Journal of Photochemistry and Photobiology C: Photochemistry Reviews, 1(1), 1-21.
vii. Gaya, U. I., & Abdullah, A. H. (2008). Heterogeneous photocatalytic degradation of organic contaminants over titanium dioxide: A review of fundamentals, progress, and problems. Journal of Photochemistry and Photobiology C: Photochemistry Reviews, 9(1), 1-12.
viii. Gogate, P. R., & Pandit, A. B. (2004). Sonophotocatalytic reactors for wastewater treatment: A critical review. AIChE Journal, 50 (5), 1051-1079.
ix. Hussein, F. H., & Abass, T. A. (2010). Photocatalytic treatment of textile industrial wastewater. International Journal of Chemical Sciences, 8(3).
x. Muruganandham, M., Suri, R., Jafari, S., Sillanpää, M., Lee, G.-J., Wu, J., & Swaminathan, M. (2014). Recent developments in homogeneous advanced oxidation processes for water and wastewater treatment. International Journal of Photoenergy.
xi. Pelaez, M., Nolan, N. T., Pillai, S. C., Seery, M. K., Falaras, P., Kontos, A. G., Dunlop, P. S., Hamilton, J. W., Byrne, J. A., & O'shea, K. (2012). A review on the visible light active titanium dioxide photocatalysts for environmental applications. Applied Catalysis B: Environmental, 125, 331-349.
xii. Thiruvenkatachari, R., Vigneswaran, S., & Moon, I. S. (2008). A review on UV/TiO2 photocatalytic oxidation process (journal review). Korean Journal of Chemical Engineering, 25(1), 64-72.
xiii. Wojnarovits, L., & Takacs, E. (2008). Irradiation treatment of azo dye containing wastewater: An overview. Radiation physics and chemistry, 77(3), 225-244.
xiv. Fujishima, A., Zhang, X., & Tryk, D. (2008). TiO2 photocatalysis and related surface phenomena. Surf Sci Rep; 63: 515-582:http://dx.doi.org/10.1016/j.surfrep.2008.10.001
xv. Cordero-Arias, L., Cabanas-Polo, S., Hao, X.G.J., Gilabert, E., Sanchez, J. A., Roether, D. W., Schubert, S., Virtanenand, A., & Boccaccini, R. (2013). Electrophoretic deposition of nanostructured-TiO2/chitosan composite coatings on stainless steel. RSC Adv.; 3: 11247-11254.

xvi. Yousefipoura, K., Akbari, A., & Bayati, M.R. (2013). The effect of EEMAO processing on surface mechanical properties of the TiO2-ZrO2 nanostructured composite coatings. Ceramics Int; 39: 7809-7815.
xvii. Mohan, L., Durgalakshmi, D., & Geetha, M., Narayanan, T.S.N.S., & Asokamani, R. (2012). Electrophoretic deposition of nanocomposites (Hap + TiO2) on titanium alloy for biomedical applications. Ceram. Int., 38, 3435-3443. DOI, 10.1016/j.ceramint.2011.12.05.
xviii. Farnoush, H., Aghazadeh Mohandesi, J., Haghshenas Fatmehsari, D., & Moztarzadeh, F. (2012). A kinetic study on the Electrophoretic Deposition of Hydroxyapatite – Titania Nanocomposite Based on a Statistical Approach, Ceram. Int., 2012, 38, 6753.
xix. Dor, S., Ruhle, S., Ofir, A., Adler, M., Grinis, L., & Zaban, A. (2009). The influence of suspension composition and deposition mode on the electrophoretic deposition of TiO2 nanoparticle agglomerates. Colloids Surf. A, 342, 70-75.
xx. Cabanas-Polo, S., & Boccaccini, A. (2015). Electrophoretic deposition of nanoscale TiO2 technology and applications. Journal of the European Ceramic society. DOI: 10.1016/j.jeurceramsoc.2015.05.03.